

The Physical Properties of HD 3651B: An Extrasolar Nemesis?

Adam J. Burgasser¹

*Massachusetts Institute of Technology, Kavli Institute for Astrophysics and Space Research,
Building 37, Room 664B, 77 Massachusetts Avenue, Cambridge, MA 02139; ajb@mit.edu*

ABSTRACT

I present detailed analysis of the near infrared spectrum of HD 3651B, a faint, co-moving wide companion to the nearby planet-hosting star HD 3651. These data confirm the companion as a brown dwarf with spectral type T8, consistent with the analysis of Luhman et al. Application of the semi-empirical technique of Burgasser, Burrows & Kirkpatrick indicates that HD 3651B has $T_{eff} = 790 \pm 30$ K and $\log g = 5.0 \pm 0.3$ for a metallicity of $[M/H] = 0.12 \pm 0.04$, consistent with a mass $M = 0.033 \pm 0.013 M_{\odot}$ and an age of 0.7–4.7 Gyr. The surface gravity, mass and age estimates of this source are all highly sensitive to the assumed metallicity; however, a supersolar metallicity is deduced by direct comparison of spectral models to the observed absolute fluxes. The age of HD 3651B is somewhat better constrained than that of the primary, with estimates for the latter ranging over ~ 2 Gyr to > 12 Gyr. As a widely orbiting massive object to a known planetary system that could potentially harbor terrestrial planets in its habitable zone, HD 3651B may play the role of Nemesis in this system.

Subject headings: Galaxy: solar neighborhood — stars: individual (HD 3651B, Gliese 570D) — stars: fundamental parameters — stars: low mass, brown dwarfs — stars: planetary systems

1. Introduction

Luhman et al. (2006) and Mugrauer et al. (2006) have recently reported the discovery of a co-moving, widely-separated ($43''$; 480 AU projected separation) companion to the

¹Visiting Astronomer at the Infrared Telescope Facility, which is operated by the University of Hawaii under Cooperative Agreement NCC 5-538 with the National Aeronautics and Space Administration, Office of Space Science, Planetary Astronomy Program.

nearby K0 V dwarf HD 3651. Low resolution near-infrared spectroscopy of this source has identified it as a late T-type brown dwarf (Luhman et al. 2006). The HD 3651 system also hosts a closely-separated ($a = 0.296 \pm 0.017$ AU), high-eccentricity ($e = 0.64 \pm 0.04$) sub-Saturn-mass planet ($M \sin i = 0.23 \pm 0.02 M_{Jupiter}$), HD 3651b, identified from radial velocity variability (Fischer et al. 2003). While several exoplanet-host stars are known to have stellar-mass companions (e.g., Lowrance, Kirkpatrick & Beichman 2002; Patience et al. 2002; Eggenberger, Udry & Mayor 2004; Raghavan et al. 2006), HD 3651ABb is the first star/brown dwarf/planet system to be identified, and is therefore a key target for studies of all three of these mass-delineated classes.

In this article, I analyze low-resolution near-infrared spectroscopy of HD 3651B, using the technique of Burgasser, Burrows & Kirkpatrick (2006, hereafter BBK) to derive the effective temperature (T_{eff}), surface gravity ($\log g$), metallicity ($[M/H]$), mass and age of this source. Acquisition and characterization of the spectral data, obtained with SpeX (Rayner et al. 2003) mounted on the 3m NASA Infrared Telescope Facility (hereafter IRTF) is described in § 2. Spectral analysis to derive the physical properties of HD 3651B is presented in § 3, with the importance of metallicity effects highlighted by the determination that this companion must be metal-rich like the system’s primary. Finally, in § 5 I speculate on the role of HD 3651B as a Nemesis analog in the HD 3651 system.

2. Observations

HD 3651B was observed with SpeX on 3 September 2006 (UT) under clear and dry conditions with good seeing ($0''.7$ at J -band). The target was acquired using the SpeX guiding camera, and low resolution near infrared spectral data were obtained using the SpeX prism mode and $0''.5$ slit, yielding a spectral resolution $\lambda/\Delta\lambda \approx 120$. The slit was aligned to the parallactic angle to mitigate differential refraction effects. Note that this setup was similar to that used by Luhman et al. (2006) for their spectral observations of HD 3651B, with the exception of a slightly narrower slit ($0''.5$ versus $0''.8$). Eight exposures of 180 s each were obtained in an ABBA dither pattern along the slit. The A0 V star HD 7215 was observed immediately afterward and at a similar airmass (1.06) for flux calibration. Internal flat field and Ar arc lamps exposures were also acquired for pixel response and wavelength calibration. All data were reduced using SpeXtool version 3.3 (Cushing, Vacca, & Rayner 2004) using standard settings (cf. Burgasser et al. 2004).

Figure 1 compares the reduced spectrum of HD 3651B to equivalent data for the T7.5 companion brown dwarf Gliese 570D (Burgasser et al. 2000) and the T8 field brown dwarf 2MASS J04151954-0935066 (Burgasser et al. 2002, hereafter 2MASS 0415-0935). The strong

H₂O and CH₄ bands present in the spectrum of HD 3651B are consistent with the observations of Luhman et al. (2006), and confirm this object as a late T-type brown dwarf. Classification of this source was done using the spectral indices of Burgasser et al. (2006). The measurements and associated subtypes are as follows: H₂O-J = 0.044 (T8), CH₄-J = 0.203 (T7.5), H₂O-H = 0.186 (T8), CH₄-H = 0.134 (T7.5) and CH₄-K = 0.043 (T8), for a mean classification of T8. This value is consistent with the T7.5 subtype derived by Luhman et al. (2006) given the typical 0.5 subtype uncertainty in near infrared T dwarf classifications (Burgasser et al. 2006).

3. The Physical Properties of HD 3651B

3.1. Derived Properties and Metallicity Dependence

As a companion to a well-studied, nearby star, the properties of HD 3651B could be readily derived by adopting the age and metallicity of the primary (e.g. Kirkpatrick et al. 2001; Wilson et al. 2001; Luhman et al. 2006). Alternately, the semi-empirical technique described in BBK can be employed. This method involves the comparison of H₂O and color spectral ratios measured on the spectrum of a late-type T dwarf, which are separately sensitive to T_{eff} and $\log g$ (for a given metallicity), to the same ratios measured on theoretical spectral models. The latter are calibrated to reproduce the measured indices for the near infrared SpeX prism spectrum of Gliese 570D (Burgasser et al. 2004), which has reported physical parameters of $T_{eff} = 782\text{--}821$ K, $\log g = 4.95\text{--}5.23$ and $[\text{Fe}/\text{H}] = 0.09 \pm 0.04$, based on empirical measurements and evolutionary models (Geballe et al. 2001; Saumon et al. 2006). This method provides constraints on both T_{eff} and $\log g$ which can then be used to infer mass and age with evolutionary models or empirically via the source’s bolometric luminosity.

In BBK and Liebert & Burgasser (2006), this method was applied assuming solar or subsolar metallicities. However, the primary of the HD 3651 has a metallicity greater than solar, $[\text{Fe}/\text{H}] = 0.12 \pm 0.04$ (Santos, Israelian & Mayor 2004). It has been shown in both BBK and Liebert & Burgasser (2006) that slightly subsolar metallicities can significantly skew the derived T_{eff} and $\log g$ values. Hence, several cases were considered for $0 \leq [\text{M}/\text{H}] \leq 0.24$. The spectral models of Burrows, Sudarsky & Hubeny (2006) were employed, spanning $700 \leq T_{eff} \leq 1100$ K, $4.5 \leq \log g \leq 5.5$ (cgs) and $0 \leq [\text{M}/\text{H}] \leq 0.5$. Four pairs of indices were compared between (H₂O-J, H₂O-H) and (K/J, K/H).¹

Figure 2 illustrates the (T_{eff} , $\log g$) phase spaces for both $[\text{M}/\text{H}] = 0$ and 0.12 over which

¹For definitions of these spectral ratios, see BBK and Burgasser et al. (2006).

the spectral ratios H₂O-J and K/H measured on the spectrum of HD 3651B match calibrated values from the models. Their intersection yields robust constraints on these parameters for the source. All four pairs of indices result in a combined $T_{eff} = 790 \pm 30$ K and $\log g = 5.0 \pm 0.2$ for $[M/H] = 0.12$ (Table 1); including the full uncertainty in $[M/H]$ increases the uncertainty on $\log g$ to 0.3 dex.² For $[M/H] = 0$, the analysis yields $T_{eff} = 810 \pm 30$ K and $\log g = 4.7 \pm 0.2$. Note that a decrease in the assumed metallicity leads to a decrease in the derived surface gravity. This is consistent with trends for subsolar metallicity T dwarfs (BBK; Liebert & Burgasser 2006), and is largely due to the impact of both metallicity and surface gravity on the relative opacity of collision-induced H₂ absorption that dominates the K-band opacity (e.g., Saumon et al. 1994).

The T_{eff} and $\log g$ values of HD 3651B for $[M/H] = 0.12 \pm 0.04$ infer $M = 0.033 \pm 0.013 M_{\odot}$ and an age $\tau = 0.7\text{--}4.7$ Gyr, based on the evolutionary models of Burrows et al. (2001). For solar metallicity, these values decrease to $M = 0.020 \pm 0.005 M_{\odot}$ and $\tau = 0.4\text{--}1.2$ Gyr, primarily due to the lower surface gravity indicated in this case. An estimate of mass can also be obtained from the bolometric luminosity (L) of HD 3651B by the relation $M = Lg/4\pi G\sigma T_{eff}^4$. Using the luminosity derived by Luhman et al. (2006), $\log L/L_{\odot} = -5.60 \pm 0.05$, and the T_{eff} and $\log g$ values derived from the spectroscopic analysis yields $M = 0.023^{+0.020}_{-0.010} M_{\odot}$ ($M = 0.011^{+0.008}_{-0.004} M_{\odot}$) for $[M/H] = 0.12$ ($[M/H] = 0.0$). These values are consistent with those derived from the evolutionary models, albeit with larger uncertainties driven primarily by the uncertainty in $\log g$.

3.2. HD 3651B: A Metal-Rich T Dwarf

The method outlined above, based on only two indices, cannot discriminate between $[M/H] = 0$ and 0.12 for HD 3651B, for in both cases it is possible to derive robust constraints on both T_{eff} and $\log g$ (this is not always the case; cf. Figure 8 of BBK). A third spectral index that is uniquely sensitive to metallicity is required, and BBK have suggested the ratio between the 1.05 and 1.25 μm peak fluxes (Y/J index) as a possible option. This ratio is sensitive to the far red wings of the pressure-broadened 0.77 μm K I doublet, and models indicate considerable metallicity sensitivity to this feature. However, the Burrows, Sudarsky & Hubeny (2006) models do not reproduce the observed trends between Y -band and J -band, likely due to current uncertainties in the treatment of the far-wing

²Note that additional systematic uncertainties of ± 50 K and ± 0.1 dex in the derived T_{eff} and $\log g$ values may be present due to uncertainty in the parameters of Gliese 570D and possible systematic effects in the spectral models (BBK).

opacities (Burrows & Volobuyev 2003; Allard et al. 2003).

An alternate procedure, used by Liebert & Burgasser (2006), is to compare the observed absolute fluxes of the brown dwarf to spectral models based on the best fit parameters for a given metallicity. This is done in Figure 3, which shows the absolute flux-calibrated spectrum of HD 3651B, based on J -band photometry from Luhman et al. (2006, 16.16 ± 0.03) and the parallax of HD 3651A from HIPPARCOS (Perryman et al. 1997, $\pi = 90.0 \pm 0.7$ mas); to predicted fluxes for two $T_{eff} = 800$ K models, one with $\log g = 4.7$ and $[M/H] = 0$ and one with $\log g = 5.0$ and $[M/H] = 0.12$. While the models provide poor fits to the 1.1 and 1.6 μm CH_4 bands, the result of well-documented deficiencies in CH_4 opacities at these wavelengths, it is clear that the lower surface gravity, solar metallicity model is too bright as compared to the data. The $[M/H] = 0.12$ model, on the other hand, provides a reasonably good match to the absolute fluxes at each of the spectral peaks. This comparison clearly supports a supersolar metallicity for HD 3651B.

Another consideration is the inferred age of HD 3651B as compared to previous age determinations for HD 3651A. Published estimates for the primary vary appreciably. Wright et al. (2004) report an age of 5.9 Gyr on the basis of weak Ca II HK emission ($\log R'_{HK} = -5.07$) and the age/activity relation of Donahue (1993). On the other hand, Rocha-Pinto et al. (2004) report a chromospheric age of only 2.1 Gyr based on a higher value of $\log R'_{HK} = -4.85$ from Soderblom et al. (1993). Indeed, a 35% variation in Ca II HK emission of HD 3651B has been seen over 17 years of observations at Mount Wilson Observatory (Duncan et al. 1991). From isochrone fitting, Nordström et al. (2004) derive a minimum age of 2.6 Gyr, Valenti & Fischer (2005) an age of 8_{-5}^{+4} Gyr and Takeda et al. (2006) a minimum age of 11.8 Gyr. While there appears to be little consensus, an older age for HD 3651A is most consistent with its chromospheric inactivity, its long rotation period (48 days; Noyes et al. 1984) and its UVW space velocities (Eggen 1989). A value in the range 2–12 Gyr is indicated.

This result again argues in favor of HD 3651B being metal-rich. The derived age for the solar metallicity case is considerably younger than that of the primary; while for $[M/H] = 0.12 \pm 0.04$, the ages of the primary and secondary overlap in the range of 2–5 Gyr. Note that this age constraint is more precise than that inferred from the primary alone, and is consistent with both components having been formed at the same time and from the same gas/dust reservoir (same age and metallicity)

There are two conclusions that may be drawn from this analysis. First, it is clear that the determination of T_{eff} and $\log g$, and hence mass and age, of an individual brown dwarf using the BBK technique is highly sensitive to the assumed metallicity, even for small

variations.³ This reflects the overall sensitivity of cool brown dwarf spectra to changes in photospheric abundances, and is not surprising given that the entire near infrared spectrum of a T dwarf is draped by atomic and molecular absorptions. While metallicity effects have been previously noted in the spectra of metal-poor T dwarfs such as 2MASS J09373487+2931409 (Burgasser et al. 2002; Knapp et al. 2004, BBK) and 2MASS J12373919+6526148 (Burgasser et al. 1999; Liebert & Burgasser 2006), it is now clear that metal-rich T dwarf spectra can also exhibit metallicity effects. These results emphasize the importance of characterizing the overall abundances — and abundance patterns — in deriving a complete and accurate characterization of a low-temperature brown dwarf. Note that HD 3651B and Gliese 570D may be a particularly useful pair in studying metallicity effects, as they appear to be identical in nearly all aspects (T_{eff} , $\log g$, age, mass and spectral energy distribution) except metallicity.

Second, it is possible that coeval brown dwarf companions may provide additional or even better constraints on the ages of their host systems than some stellar primaries. While age estimates for stars on the basis of chromospheric activity and kinematics can vary appreciably, and are less discriminating at later ages, the example of HD 3651B demonstrates that a late-type brown dwarf can potentially be age-dated with higher precision. However, the accuracy of these ages remains unclear, as they are tied to both the fidelity of evolutionary models and, in the case of the BBK technique, the accuracy and calibration of spectral models. In the former case, there have been few empirical checks on the evolutionary models of brown dwarfs at late ages,⁴ although BBK found consistency between the radii of field T dwarfs empirically derived from luminosity measurements and those based on evolutionary models. In the latter case, there appears to be consistency between different sets of spectral models, as an equivalent analysis of the spectrum of HD 3651B using the COND models of Allard et al. (2001) produced nearly identical results. Hence, at first glance it appears that late-type brown dwarf companions could be useful sources for characterizing the properties of a presumably coeval system, although further empirical tests of brown dwarf evolutionary models are needed.

³[M/H] = 0.12 implies only a 32% increase in metal abundance over solar.

⁴At very young ages ($\sim 1\text{--}5$ Myr), both Mohanty et al. (2004) and Stassun, Mathieu & Valenti (2006) have found discrepancies between evolutionary models and observed parameters. It is possible that these discrepancies arise from the initial conditions assumed in the evolutionary models, and may be unimportant at late ages (cf. Marley et al. 2006).

4. HD 3651B: An Extrasolar Nemesis?

HD 3651B is the first wide brown dwarf companion found in a system hosting at least one known planet. This raises an intriguing question: how has the evolution of the HD 3651 planetary system — and specifically the development of life on any putative habitable planets in this system — been influenced by this distant brown dwarf companion? This speculative question is an appropriate one, as putative terrestrial bodies within a portion of HD 3651A’s habitable zone (Kasting, Whitmire & Reynolds 1993) can persist without dynamical disruption by HD 3651b (Jones, Underwood & Sleep 2005), even considering this giant planet’s probable inward migration (Mandell & Sigurdsson 2003). Terrestrial planet formation around the primary of a wide binary system has also been shown to be feasible (Holman, & Wiegert 1997; Quintana 2004). However, the formation, existence and habitability of terrestrial planets in the HD 3651 system may be inhibited by dynamical perturbations from HD 3651B, both directly through orbital modulation⁵ (Takeda & Rasio 2005); or the scattering of small bodies, resulting in sustained impacting onto the planet’s surface. Yet terrestrial planets on mildly eccentric orbits can maintain habitability depending on the properties of their atmospheres (Adams & Laughlin 2006), while increased impacting rates may in fact facilitate the emergence of life. In the case of the Earth, the late heavy bombardment period between 4.5 and 3.8 Gyr ago resulted in one particularly cataclysmic impact that formed the Moon (Hartmann & Davis 1975), whose tidal forces have maintained Earth’s tilt to the Sun and have thereby reduced climate variation. Impacts of icy bodies may have brought necessary water ice to Earth’s surface (Chyba 1987; Delsemme 1998) as well as chemical precursors to biotic life (Chyba et al. 1990). On the other hand, later impacts clearly have a negative effect on the evolution of macrobiotic life (Alvarez et al. 1980; Hildebrand et al. 1991).

As an instigator of planetary impacts, HD 3651B may play the role of Nemesis in the HD 3651 system. This hypothesized companion to the Sun (Davis, Hut & Muller 1984; Whitmire & Jackson 1984) has been proposed to explain apparent periodicities in massive extinctions (Fischer & Arthur 1977; Raup & Sepkoski 1984; Hut et al. 1987), terrestrial cratering rates (Alvarez & Muller 1984; Rampino & Stothers 1984), reversals of Earth’s magnetic fields (Raup 1985) and, more recently, the peculiar orbits of inner Oort Cloud planetoids (Brown, Trujillo & Rabinowitz 2004; Gaudi & Bloom 2005). If HD 3651B were present at its observed separation but bound to the Sun, it would be invisible to the naked eye ($M_V \sim 27$ implies $V \sim 9$) but readily detectable by Hipparcos, Tycho (Perryman et al.

⁵Indeed, Luhman et al. 2006 suggest that the eccentricity of HD 3651b may be driven by secular perturbations from HD 3651B.

1997) and early wide-field near-infrared sky surveys ($K \sim -1$; cf. the Two-Micron Sky Survey, Neugebauer & Leighton 1969). If HD 3651B was at the distance from the Sun proposed for Nemesis ($\sim 1.5 \times 10^5$ AU; Davis, Hut & Muller 1984), it would be invisible on visual photographic plate images ($V \sim 20$) but a relatively bright source ($J \sim 10$) in the Two Micron All Sky Survey (Skrutskie et al. 2006).

Searches for a solar Nemesis have so far turned up negative (e.g., Perlmutter 1986). However, as widely-separated low mass stellar companions appear to be prevalent in known planet-hosting systems (e.g., Raghavan et al. 2006), and with widely-separated brown dwarf companions to these systems only now being identified, Nemesis counterparts may be a common facet of all planetary systems and an important consideration for the emergence of terrestrial-based life.

The author thanks D. Chakrabarty and J. Winn for their helpful comments on an early version of the manuscript, and acknowledges the support of telescope operator E. Volquardsen and instrument specialist J. Rayner during the IRTF observations. The author also thanks the anonymous referee for her/his insightful comments that led to the investigation of metallicity effects in the $T_{eff}/\log g$ analysis. Electronic versions of their evolutionary and spectral models were kindly provided by A. Burrows and P. Hauschildt for this work. The author wishes to recognize and acknowledge the very significant cultural role and reverence that the summit of Mauna Kea has always had within the indigenous Hawaiian community. He is most fortunate to have had the opportunity to conduct observations from this mountain.

Facilities: IRTF(SpeX)

REFERENCES

- Adams, F. C., & Laughlin, G. 2006, *ApJ*, 649, 992
- Allard, F., Hauschildt, P. H., Alexander, D. R., Tamanai, A., & Schweitzer, A. 2001, *ApJ*, 556, 357
- Allard, N. F., Allard, F., Hauschildt, P. H., Kielkopf, J. F., & Machin, L. 2003, *A&A*, 411, L473
- Alvarez, L. W., Alvarez, W., Asaro, F., & Michel, H. V. 1980, *Science*, 208, 1095
- Alvarez, W., & Muller, R. A. 1984, *Nature*, 308, 718

- Brown, M. E., Trujillo, C., & Rabinowitz, D. 2004, *ApJ*, 617, 645
- Burgasser, A. J., Burrows, A., & Kirkpatrick, J. D. 2006, *ApJ*, 639, 1095 (BBK)
- Burgasser, A. J., McElwain, M. W., Kirkpatrick, J. D., Cruz, K. L., Tinney, C. G., & Reid, I. N. 2004, *AJ*, 127, 2856
- Burgasser, A. J., Geballe, T. R., Leggett, S. K., Kirkpatrick, J. D., & Golimowski, D. A. 2006, *ApJ*, 637, 1067
- Burgasser, A. J., et al. 1999, *ApJ*, 522, L65
- Burgasser, A. J., et al. 2000, *ApJ*, 531, L57
- Burgasser, A. J., et al. 2002, *ApJ*, 564, 421
- Burrows, A., Hubbard, W. B., Lunine, J. I., & Liebert, J. 2001, *Rev. of Modern Physics*, 73, 719
- Burrows, A., Sudarsky, D., & Hubeny, I. 2006, *ApJ*, 640, 1063
- Burrows, A., & Volobuyev, M. 2003, *ApJ*, 583, 985
- Chyba, C. F. 1987, *Nature*, 330, 632
- Chyba, C. F., Thomas, P. J., Brookshaw, L., & Sagan, C. 1990, *Science*, 249, 366
- Cushing, M. C., Vacca, W. D., & Rayner, J. T. 2004, *PASP*, 116, 362
- Davis, M., Hut, P., & Muller, R. A. 1984, *Nature*, 308, 715
- Delsemme, A. H. 1998, *P&SS*, 47, 125
- Donahue, R. A. 1993, Ph.D. Thesis, New Mexico State University
- Duncan, D. K., et al. 1991, *ApJS*, 76, 383
- Eggen, O. J. 1989, *PASP*, 101, 366
- Eggenberger, A., Udry, S., & Mayor, M. 2004, *A&A*, 417, 353
- Fischer, A. G., & Arthur, M. A. 1977, *Soc. Econ. Paleont. Miner. Spec. Publ.* 25, 19
- Fischer, D. A., Butler, R. P., Marcy, G. W., Vogt, S. S., & Henry, G. W. 2003, *ApJ*, 590, 1081

- Gaudi, B. S., & Bloom, J. S. 2005, *ApJ*, 635, 711
- Geballe, T. R., Saumon, D., Leggett, S. K., Knapp, G. R., Marley, M. S., & Lodders, K. 2001, *ApJ*, 556, 373
- Hartmann, W. K., & Davis, D. R. 1975 *Icarus*, 24, 505
- Hildebrand, A. R., Penfield, G. T., Kring, D. A., Pilkington, M., Camargo, A. Z., Jacobsen, S. B., & Boynton, W. V. et al. 1991, *Geology*, 19, 867
- Holman, M., & Weigert, P. A. 1997, *AJ*, 117, 621
- Hut, P., Alvarez, W., Elder, W. P., Kauffman, E. G., Hansen, T., Keller, G., Shoemaker, E. M., & Weissman, P. R. 1987, *Nature*, 329, 118
- Jones, B. W., Underwood, D. R., & Sleep, P. N. 2005, *ApJ*, 622, 1091
- Kasting, J. F., Whitmire, D. P., & Reynolds, R. T. 1993, *Icaurs*, 101, 108
- Kirkpatrick, J. D., Dahn, C. C., Monet, D. G., Reid, I. N., Gizis, J. E., Liebert, J., & Burgasser, A. J. 2001, *AJ*, 121, 3235
- Knapp, G., et al. 2004, *ApJ*, 127, 3553
- Liebert, J., & Burgasser, A. J. 2006, *ApJ*, in press
- Lowrance, P. J., Kirkpatrick, J. D., & Beichmann, C. A. 2002, *ApJ*, 572, L79
- Luhman, K. L., et al. 2006, *ApJ*, in press
- Mandell, A. M., & Sigurdsson, S. 2003, *ApJ*, 599, L111
- Marley, M. S., Fortney, J. J., Hubickyj, O., Bodenheimer, P., & Lissauer, J. J. 2006, *ApJ*, in press
- Mohanty, S., Basri, G., Jayawardhana, R., Allard, F., Hauschildt, P., & Ardila, D. 2004, *ApJ*, 609, 854
- Mugrauer, M., Seifahrt, A., Neuhäuser, R., & Mazeh, T. 2006, *MNRAS*, in press
- Neugebauer, G., & Leighton, R. B. 1969, *Two-Micron Sky Survey, A Preliminary Catalogue* (Washington: NASA)
- Nordström, B., et al. 2004, *A&A*, 418, 989

- Noyes, R. W., Hartmann, L. W., Baliunas, S. L., Duncan, D. K., & Vaughan, A. H. 1984, *ApJ*, 279, 763
- Patience, J., et al. 2002, *ApJ*, 581, 654
- Perlmutter, S. 1986, Ph.D. Thesis, University of California, Berkeley
- Perryman, M. A. C., et al. 1997, *A&A*, 323, L49
- Quintana, E. V. 2004, Ph.D. Thesis, University of Michigan
- Raghavan, D., Henry, T. J., Mason, B. D., Subasavage, J. P., Jao, W.-C., Beaulieu, T. D., & Hambly, N. C. 2006, *ApJ*, 646, 523
- Rampino, M. R., & Strothers, R. B. 1984, *Nature*, 308, 709
- Raup, D. M. 1985, *Nature*, 314, 341
- Raup, D. M., & Sepkoski, J. J. 1984, *Proc. Nat. Acad. Sci. USA*, 81, 801
- Rayner, J. T., Toomey, D. W., Onaka, P. M., Denault, A. J., Stahlberger, W. E., Vacca, W. D., Cushing, M. C., & Wang, S. 2003, *PASP*, 155, 362
- Rocha-Pinto, H. J., et al. 2004, *A&A*, 423, 517
- Santos, N. C., Israelian, G., & Mayor, M. 2004, *A&A*, 415, 1153
- Saumon, D., Bergeron, P., Lunine, J. I., Hubbard, W. B., & Burrows, A. 1994, *ApJ*, 424, 333
- Saumon, D., Marley, M. S., Cushing, M. C., Leggett, S. K., Roellig, T. L., Lodders, K., & Freedman, R. S. 2006, *ApJ*, in press.
- Soderblom, D. R., Stauffer, J. R., , Hudon, J. D., & Jones, B. F. 1993, *ApJS*, 85, 315
- Skrutskie, M. F., et al. 2006, *AJ*, 131, 1163
- Stassun, K. G., Mathieu, R. D., & Valenti, J. A. 2006, *Nature*, 440, 311
- Takeda, G., Ford, E. B., Sills, A., Rasio, F. A., Fischer, D. A., & Valenti, J. A. 2006, *ApJS*, submitted
- Takeda, G., & Rasio, F. A. 2005, *ApJ*, 627, 1001
- Valenti, J. A., & Fischer, D. A. 2005, *ApJS*, 159, 141

Whitmire, D. R., & Jackson, A. A. 1984, *Nature*, 308, 713

Wilson, J. C., Kirkpatrick, J. D., Gizis, J. E., Skrutskie, M. F., Monet, D. G., & Houck, J. R. 2001, *AJ*, 122, 1989

Wright, J. T., Marcy, G. W., Butler, R. P., & Vogt, S. S. 2004, *ApJS*, 152, 261

Table 1. Derived Physical Properties of HD 3651B.

Parameter	[M/H] = 0.00	[M/H] = 0.08	[M/H] = 0.12 ^a	[M/H] = 0.16	[M/H] = 0.24
T_{eff} (K)	810±30	790±30	790±30	790±30	780±40
$\log g$ (cgs)	4.7±0.2	4.9±0.2	5.0±0.2	5.0±0.2	5.2±0.2
Mass (M_{\odot})	0.020±0.005	0.027±0.007	0.032±0.008	0.035±0.011	0.047±0.013
Age (Gyr)	0.4–1.2	0.7–2.8	1.0–3.7	1.0–4.7	2.6–9.3

^aSantos, Israelian & Mayor (2004) derive a metallicity for the primary of $[\text{Fe}/\text{H}] = 0.12 \pm 0.04$.

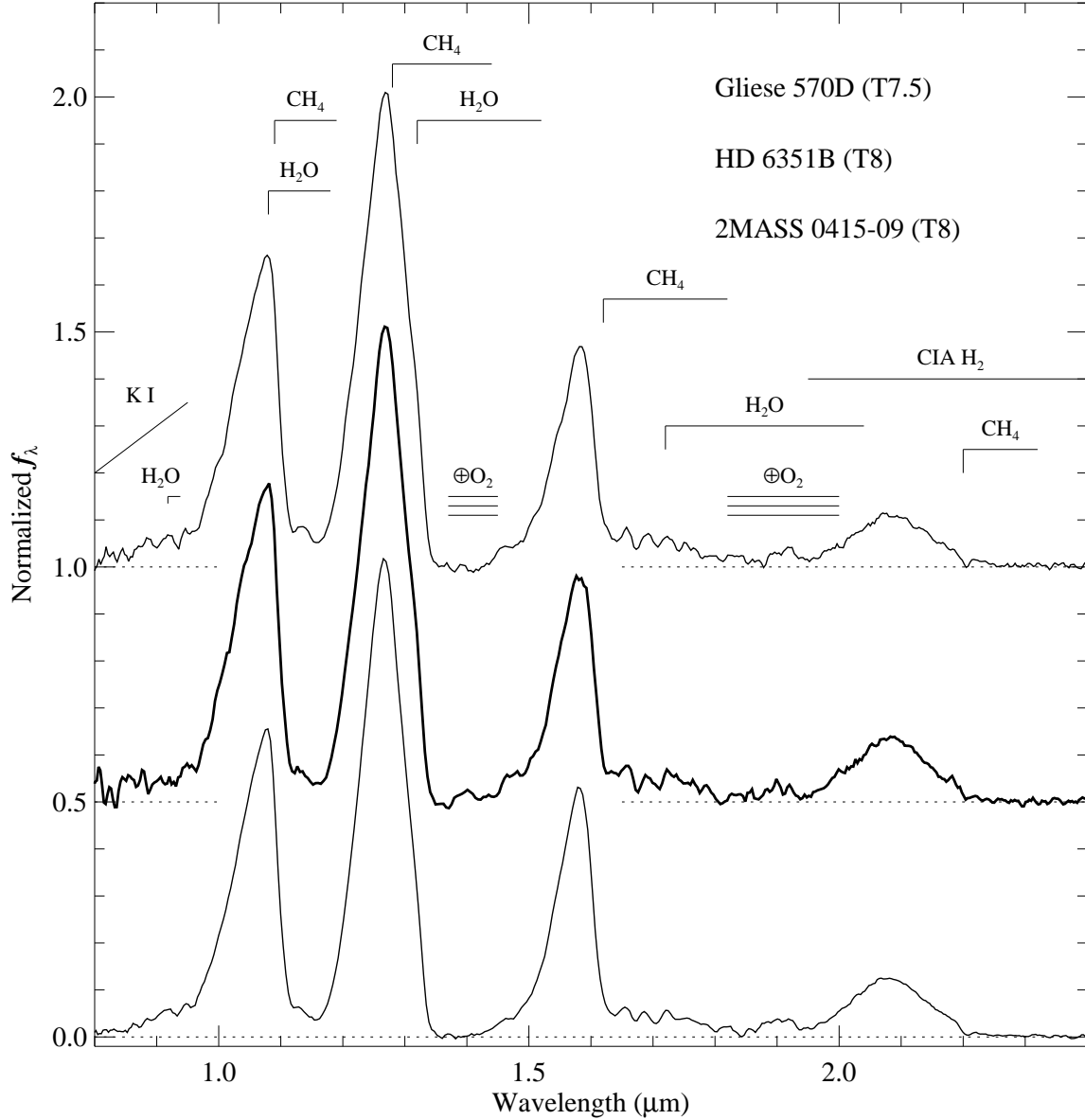


Fig. 1.— From top to bottom, normalized near-infrared spectra of the T7.5 companion Gliese 570D, HD 3651B and the T8 field brown dwarf 2MASS 0415-0935, all obtained with SpeX on IRTF. All spectra are normalized at $1.27 \mu\text{m}$ and offset by constants (dotted lines). Major spectral features are noted; the \oplus symbols designate regions of strong telluric absorption.

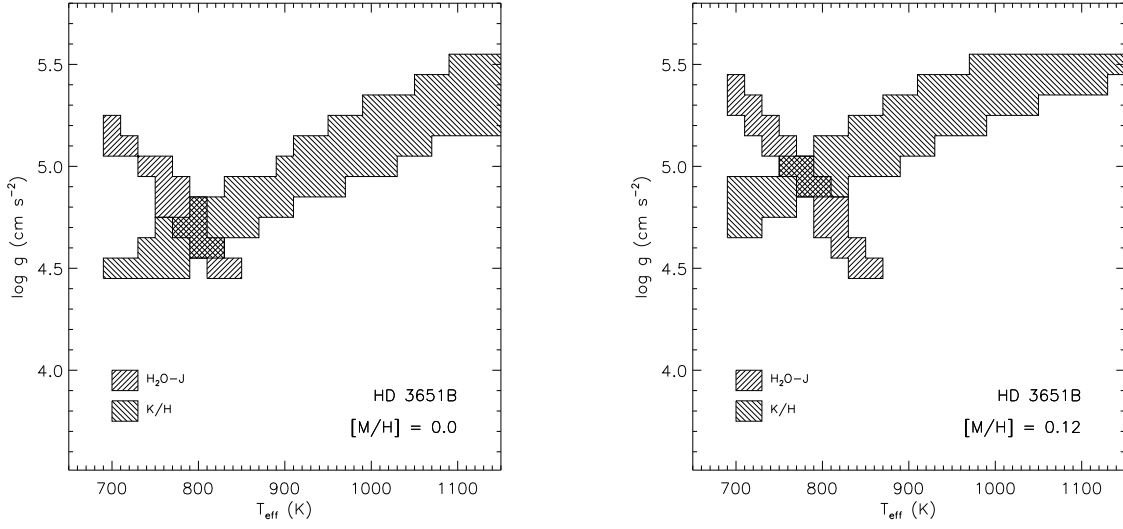


Fig. 2.— Phase spaces of T_{eff} and $\log g$ constrained for HD 3651B by the indices $\text{H}_2\text{O-J}$ and K/H using the technique of BBK for metallicities $[M/H] = 0.0$ (left) and 0.12 (right). Model indices are measured from calculations by Burrows, Sudarsky & Hubeny (2006) and calibrated to observations of Gliese 570D. The intersecting cross-hatched regions provide robust constraints on T_{eff} and $\log g$. Note the higher gravity constraint derived for the higher metallicity (see also Table 1).

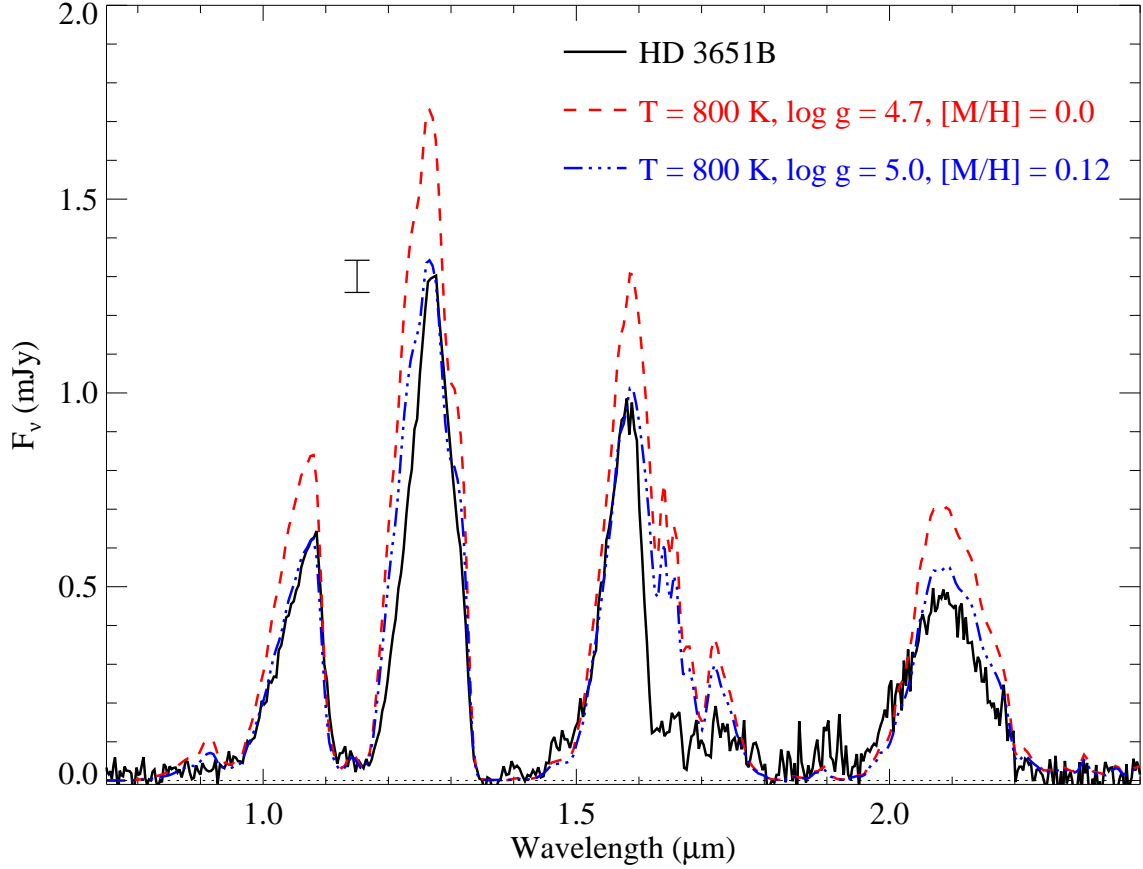


Fig. 3.— Comparison of the absolute flux-calibrated spectrum of HD 3651B (black line) to two $T_{eff} = 800$ K spectral models from Burrows, Sudarsky & Hubeny (2006): $\log g = 4.7$ and $[M/H] = 0.0$ (red dashed line), and $\log g = 5.2$ and $[M/H] = 0.12$ (blue triple-dot dashed line). Flux calibration of the HD 3651B spectrum is based on J -band photometry from Luhman et al. (2006, 16.16 ± 0.03) and the parallax of the primary as measured by HIPPARCOS (Perryman et al. 1997, $\pi = 90.0 \pm 0.7$ mas). Uncertainty in this calibration at the J -band peak is indicated by the error bar. Note the agreement between the data and the $[M/H] = 0.12$ model.